14th International Symposium on Turbulence and Shear Flow Phenomena (TSFP14)
Heidelberg, Germany, July 28–31, 2026

SCALE-DEPENDENT CONVECTION VELOCITIES OF PASSIVE SCALAR STRUCTURES IN WALL-BOUNDED TURBULENCE

Christian Dederichs — Jonathan Neuhauser — Davide Gatti
Institute of Fluid Mechanics
Karlsruhe Institute of Technology
Kaiserstr. 10, 76131 Karlsruhe, Germany
davide.gatti@kit.edu

ABSTRACT

The convection velocity of turbulent structures is central to Taylor's hypothesis and to the interpretation of time-resolved measurements in wall-bounded turbulence. While the convection behaviour of velocity fluctuations has been studied extensively, much less is known about passive scalar fluctuations, despite their relevance to temperature-based wall-shear-stress estimation and heat-transfer modelling. In the present work, the scale-dependent convection velocity of passive scalar structures is analysed in turbulent plane channel flow by extending the residual-minimisation approach of del Álamo & Jiménez (2009) to the passive scalar transport equation. Direct numerical simulations of doubly periodic channel flows are performed at friction Reynolds numbers $Re_\tau = 180,\ 500,\ 1000$, while passive scalars with Prandtl numbers $Pr = 0.025,\ 0.4,\ 1$ are considered. The results show that the global convection velocity of passive scalar fluctuations approaches the local mean streamwise velocity away from the wall, but tends to a finite near-wall value that increases as Pr decreases. This behaviour is linked to the stronger contribution of large, fast-convecting structures in low-Pr flows. A scale-resolved analysis further shows that larger scalar structures convect at velocities closer to the bulk velocity, whereas smaller scales are more strongly influenced by the local mean flow. In addition, the near-wall convection behaviour is found to deviate from previously proposed empirical scaling laws for $Pr < 1$ and to exhibit a measurable Reynolds-number dependence. These findings improve the physical understanding and modelling of passive-scalar convection in wall turbulence and support the development of thermographic methods for indirect wall-friction estimation.

INTRODUCTION

In wall-bounded turbulent flows, such as plane channels, pipe flows and boundary layers, the idea that turbulence-fluctuation patterns on a plane parallel to the wall are primarily advected downstream while remaining approximately unaltered dates back to Taylor's frozen-turbulence hypothesis Taylor (1938). In mathematical form, the hypothesis states that the material derivative of a flow quantity $q(x,t)$ is approximately zero:

$$\frac{\partial q(x,t)}{\partial t} \approx -U_{\mathrm{c},q}\frac{\partial q(x,t)}{\partial x}, \tag{1}$$

where $U_{\mathrm{c},q}$ is the so-called *convection velocity*, i.e. the average velocity at which fluctuation patterns of q are convected downstream along the streamwise coordinate x, and t denotes time.

Taylor's hypothesis in the form of equation (1) plays a central role in the study of wall-bounded turbulence (Taylor, 1938; Moin, 2009). It is ubiquitously applied to convert temporal fluctuation histories, such as those typically acquired via hot-wire anemometry in laboratory experiments, into spatial ones. Conversely, spatial fluctuation data, such as those obtained from flow snapshots in numerical simulations, can be converted into temporal signals, which are more difficult to obtain numerically. Then, the convection velocity $U_{\mathrm{c},q}$ is closely related to the evolution and propagation of the turbulent eddies that populate wall-bounded turbulent flows and is therefore linked to several important properties of such flows. Most notably, $U_{\mathrm{c},q}$ in the immediate vicinity of walls has been observed to be proportional to wall friction (Jeon *et al.*, 1999; Quadrio & Luchini, 2003) and is therefore used as a proxy for developing indirect convection-velocity-based measures of wall shear stress (see, e.g. Miozzi & Costantini (2021)), a quantity that is typically difficult to measure directly.

Retrieving convection velocities is challenging even at a theoretical level, as the Taylor hypothesis in equation (1) holds only approximately. Several convection velocity definitions can be thought of and many propositions have been suggested in the literature, all focussing on slightly different aspects of the actual physical flow behaviour (Hussain & Clark, 1980; Goldschmidt *et al.*, 1981). Two main approaches exist in the literature: one based on space-time cross-correlations and one based on minimising the residual of the Taylor hypothesis itself. Loosely speaking, with the cross-correlation method $U_{\mathrm{c},q}$ is obtained as $U_{\mathrm{c},q} = \Delta x_{\max}/\Delta t$ by shifting two consecutive spatial wall fluctuation patterns separated by a time lag Δt along the x-direction by an amount $\Delta x_{\max}$, which maximises the correlation between them. This procedure has been widely used to determine the convection velocity of velocity fluctuations (Quadrio & Luchini, 2003; Kim & Hussain, 1993). Well-known limitations are the sensitivity to spatial and temporal resolutions, placing stringent requirements on numerical and experimental data, and the requirement for a clearly defined streamwise direction, along which the celerity is evaluated.

A more general physics-based approach (del Álamo & Jiménez, 2009) relies on the Taylor hypothesis of equation (1): $U_{\mathrm{c},q}$ is determined as the one, for which the hypothesis applies the best, i.e. which yields the minimum residuum in the least square sense. This method, first applied to numerical data of turbulent channel flows by del Álamo & Jiménez (2009) provides several advantages. The residual of equation (1) quantifies how well the Taylor hypothesis holds through, thereby assessing the well-posedness of $U_{c,q}$. When all terms in the governing equations for q are available, the temporal derivative can be replaced, enabling the estimation of $U_{c,q}$ from spatial information of a single flow snapshot. This also allows examination of the contribution of individual physical mechanisms (terms in the governing equations) to the convection velocity.

However measured, $U_{c,q}$ was shown to be dependent on many factors such as the distance to a solid surface in wall-bounded flows (Kim & Hussain, 1993; Quadrio & Luchini, 2003), dimensionless numbers, e.g. *Re* (Romano, 1995; Khoo *et al.*, 2001), or the characteristic size of the considered turbulent fluctuation represented by its wavenumber vector $\boldsymbol{k}$ in Fourier-space (Wills, 1964; Choi & Moin, 1990; Jeon *et al.*, 1999; Renard & Deck, 2015). Especially the latter is an important aspect, for example, in the modelling of spatial turbulence spectra from temporal ones (Cui & Jacobi, 2024), as neglecting the scale-dependence of $U_{c,q}$ is shown to lead to large errors (Zaman & Hussain, 1981). Convection velocity definitions taking this scale dependence into account generally require spectral information in both the spatial and the temporal directions (Wills, 1964; Hussain & Clark, 1980) and are thus hard to measure in both numerical and laboratory experiments. As a result, information on the scale dependence of convection velocities from literature besides the work by del Álamo & Jiménez (2009) is rare, it focuses mostly on the propagation of velocity fluctuations and thus do not consider passive scalars, such as those employed to represent small temperature fluctuations.

Understanding the behaviour of the convection velocity of temperature fluctuations is extremely relevant, for example, for the development of novel temperature-based indirect measurement of skin friction (Miozzi & Costantini, 2021) and for the modelling of conjugate heat transfer (Hetsroni *et al.*, 2004). Furthermore, the influence of the Prandtl number on the convection velocities of temperature fluctuations has only been studied to a small extent (Kowalewski *et al.*, 2003; Hetsroni *et al.*, 2004; Liu *et al.*, 2023), and lacks the dependence on different turbulent scales, which remains largely unexplored. With the aim of making first steps in filling this gap, the present work exploits direct numerical simulations (DNSs) of plane channel flow to address the scale-dependent convection velocity of temperature fluctuations in turbulent channels at different Reynolds *Re* and Prandtl *Pr* numbers, applying for the first time the approach by del Álamo & Jiménez (2009) to the temperature equation.

NUMERICAL METHODS

The doubly-periodic turbulent channel with its geometric dimensions in the x (streamwise), the y (wall-normal), and the z (spanwise) direction are shown in figure 1 together with the respective velocity components U, V, and W. Besides the equations for mass and momentum transport, additional transport equations for passive scalars are solved with the spectral solver Fast&Fourier based on the algorithms described by Luchini & Quadrio (2005). Both the streamwise velocity components and the passive scalars are driven by setting their respective bulk values to unity in every time iteration by means of homogeneous forcing (Pirozzoli *et al.*, 2016). The passive scalars and velocity are set to vanish at the walls of the channel. Three simulation cases are conducted with friction Reynolds numbers $Re_\tau = u_\tau h/\nu =\in \{180,\ 500,\ 1000\}$, defined by the friction velocity u_τ, the channel half-width h, and the fluid kinematic viscosity ν. In each simulation, passive scalars with Prandtl numbers $Pr = \nu/a =\in \{0.025,\ 0.4,\ 1\}$ are considered, where a is the thermal diffusivity. Statistically independent flow snapshots are saved and later used for evaluation of the convection velocities, which we compute for both the velocity and temperature fluctuations. The convection velocities are computed with the method by del Álamo & Jiménez (2009), here extended to passive scalars for the first time. Accordingly, the convection velocity $u_{c,\Theta}$ of passive scalar (Θ) fluctuations of a given streamwise and spanwise wavenumber — denoted respectively as k_x and k_z — is computed as:

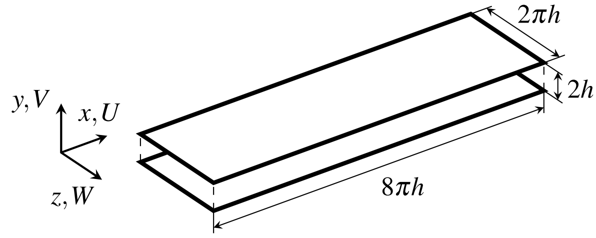

Figure 1. DNS configuration of plane channel flow

$$u_{c,\Theta}(k_x,k_z,y) := -\frac{\mathrm{Im}\left[\left\langle \widehat{\theta}^* \frac{\partial \widehat{\theta}}{\partial t} \right\rangle\right]}{k_x \left\langle \widehat{\theta}^* \widehat{\theta} \right\rangle}\,, \tag{2}$$

where $\langle \cdot \rangle$ indicates the ensemble average and $\theta := \Theta - \langle\Theta\rangle$ is the passive scalar fluctuation. The Fourier coefficient of a quantity is indicated by $\widehat{(\cdot)}$, while $(\cdot)^*$ denotes it's complex-conjugate.

The global mean convection velocity is defined as (del Álamo & Jiménez, 2009):

$$U_{c,\Theta}(y) := \frac{\iint_{\mathscr{K}} u_{c,\Theta} k_x^2 \widehat{\theta}^* \widehat{\theta}\ \mathrm{d}k_x \mathrm{d}k_z}{\iint_{\mathscr{K}} k_x^2 \widehat{\theta}^* \widehat{\theta}\ \mathrm{d}k_x \mathrm{d}k_z} \tag{3}$$

as a weighted average of $u_{c,\Theta}$ over a wavenumber (sub)set $\mathscr{K}$. This quantity is closely related to the typical (non-scale-dependent) convection velocity definitions found in the literature (Hussain & Clark, 1980; Kim & Hussain, 1993; Quadrio & Luchini, 2003).

RESULTS

Global convection velocity

In figure 2, the global convection velocities of passive scalar fluctuation at different Prandtl numbers are shown as function of the wall distance. The space of *all* wavenumbers is considered for $\mathscr{K}$ in equation (3). The subfigures show the results of the simulations at $Re_\tau \approx 180$, $Re_\tau \approx 500$, and $Re_\tau \approx 1000$, from left to right. The mean streamwise velocity $\langle U\rangle$ and the bulk velocity U_b are shown for comparison, and viscous scaling (based on u_τ and ν) is applied to all quantities and denoted with the superscript '+'.

The convection velocity $U^+_{c,\Theta}$ for $Pr = 1$ closely resemble $U^+_{c,u}$, the one for the streamwise velocity fluctuations (not shown). While $U^+_{c,\Theta}$ at all *Pr* tends to be close to (but slightly smaller than) the mean streamwise velocity towards the channel centre, different-*Pr* clearly show different convection behaviour closer to the wall. As already observed for $U^+_{c,u}$

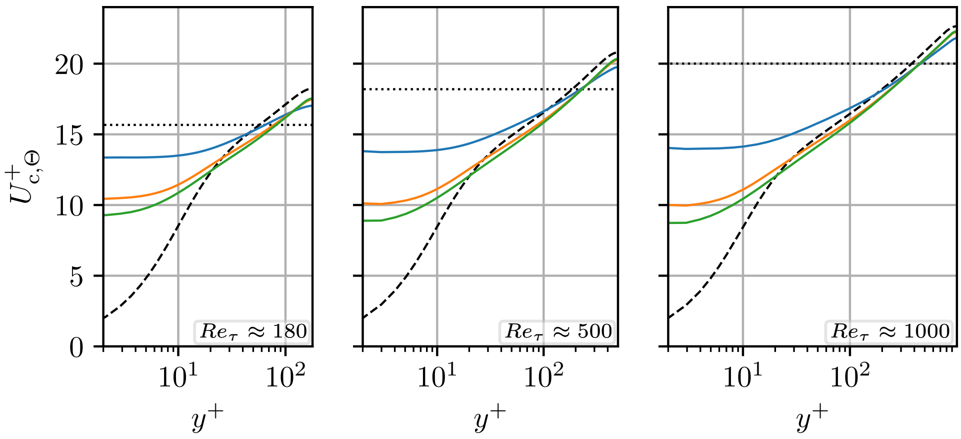

Figure 2. Overall convection velocities of passive scalar fluctuations with respect to wall distance in viscous units at ——, $Pr = 0.025$; ——, $Pr = 0.4$; ——, $Pr = 1$. Also shown for reference are the respective values of ⋯⋯, U^+_b; - - - , $\langle U^+\rangle$.

(Quadrio & Luchini, 2003; del Álamo & Jiménez, 2009), also $U^+_{c,\Theta}$ becomes constant and is nonzero in proximity of the wall, a feature typically attributed to the footprint of turbulent eddies farther from the wall, mainly residing within the buffer layer, inducing fluctuation on the near-wall layer. With a decrease in the Pr-number, larger values of $U^+_{c,\Theta}$ can be observed close to the wall, while this relationship is inverted at the channel centre. Qualitatively, this can be attributed to the larger characteristic lengthscales of passive scalar fluctuations in low-Pr flows. Since large structures occupy larger areas of the turbulent channel and they can be assumed to advect downstream at a speed similar to the mean velocity at their baricenter, their convection velocities become closer to the bulk velocity. Smaller structures on the other hand are strongly localised and their convection velocity thereby closely related to $\langle U\rangle$. This is most clearly observed for $Pr = 0.025$, where $U^+_{c,\Theta}$ is the largest of all passive scalars at the wall (where $U^+_b > \langle U^+\rangle$) and the smallest at the channel centre (where $U^+_b < \langle U^+\rangle$). Additionally, we observe that the wall distance at which curves of $U^+_{c,\Theta}$ at different Pr cross each other gets for increasing Re closer and closer to the y^+, at which $\langle U^+\rangle$ becomes larger than U^+_b.

The constant near-wall value taken by $U^+_{c,\Theta}$ is particularly relevant due to its relationship to the wall shear stress τ_w in canonical wall-bounded flows, which may be exploited to infer friction (Liu & Woodiga, 2011; Miozzi & Costantini, 2021) from time-resolved thermographic measurements (Liu *et al.*, 2021; Astarita & Carlomagno, 2012) of wall temperature fluctuations. Currently, the only work systematically investigating the wall value of $U^+_{c,\Theta}$ at different Pr-numbers is the one by Hetsroni *et al.* (2004), who addressed $U^+_{c,\Theta}$ in turbulent open-channel flows at $Re_\tau = 171$ and $Pr \in \{1,\ 5.4,\ 54\}$. Hetsroni *et al.* (2004) proposes that the near-wall value of $U^+_{c,\Theta}$ for a constant temperarture wall is directly proportional to the one taken by $U^+_{c,u}$, which is approximately $U^+_{c,u} \approx 10$, according to the following empirical relationship:

$$U_{c,\Theta} \approx \frac{U_{c,u}}{Pr^{\frac{1}{3}}} \quad \text{(near the wall).} \tag{4}$$

Figure 3 shows the near-wall ($y^+ < 2$) ratio $U^+_{c,\Theta}/U^+_{c,u}$ as function of the Pr-number, and compares the data by Hetsroni *et al.* (2004) and the proposed scaling law (4) with the present data at different Re-numbers. As is evident from figure 3, the values of the lower Pr number scalars do *not* follow the trend

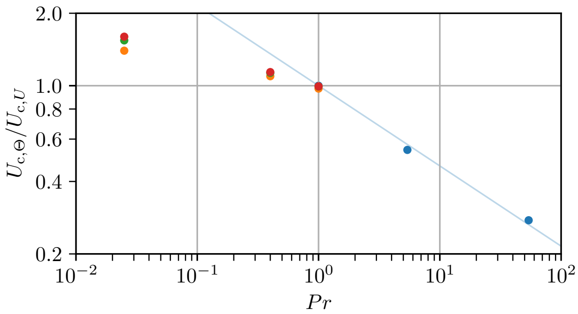

Figure 3. Dependence of the overall convection velocities of passive scalar structures on the Prandtl number in close vicinity to the wall. Depicted cases are •, $Re_\tau \approx 171$ (Hetsroni *et al.*, 2004); •, $Re_\tau \approx 180$; •, $Re_\tau \approx 500$; •, $Re_\tau \approx 1000$. Also shown for reference is ——, equation 4 (Hetsroni *et al.*, 2004)

proposed by Hetsroni *et al.* (2004): $U_{c,\Theta}/U_{c,U}$ is significantly smaller than $1/Pr^{1/3}$ for all the considered cases with $Pr < 1$.

The effect of changing Reynolds number on $U^+_{c,\Theta}$ is limited overall, but it measurably affects the constant value approached in the wall vicinity and becomes increasingly important for decreasing Pr-numbers. This effect can be explained by considering the fluctuation energy spectra and the scale-dependent convection velocities, as will be done in the upcoming section.

Convection velocity at different lengthscales

The definitions given in equations (2) and 3 allow to assess the convection velocity of Θ fluctuations occurring at different characteristic lenghtscales. On the one hand, $u^+_{c,\Theta}(k_x, k_z, y)$ can be computed via equation (2) as function of the wavenumbers k_x and k_z representing the two statistically homogeneous directions, and the wall-normal distance. On the other, equation (3) can be employed, as done for the overall convection velocity, albeit with a suitable definition of the integration domain $\mathscr{K}$, in order to assess the convection velocity across a specific range of scales. In the following, both approaches are pursued, starting from the latter.

A scale-dependent convection velocity, which we indicate with $U^+_{c,\Theta}(\lambda, y)$, is computed as a function of the isotropic lengthscale $\lambda^+ = 2\pi/k^+$ and the wall-normal distance y^+ by integrating (3) over a domain $\mathscr{K}$ encompassing a circu-

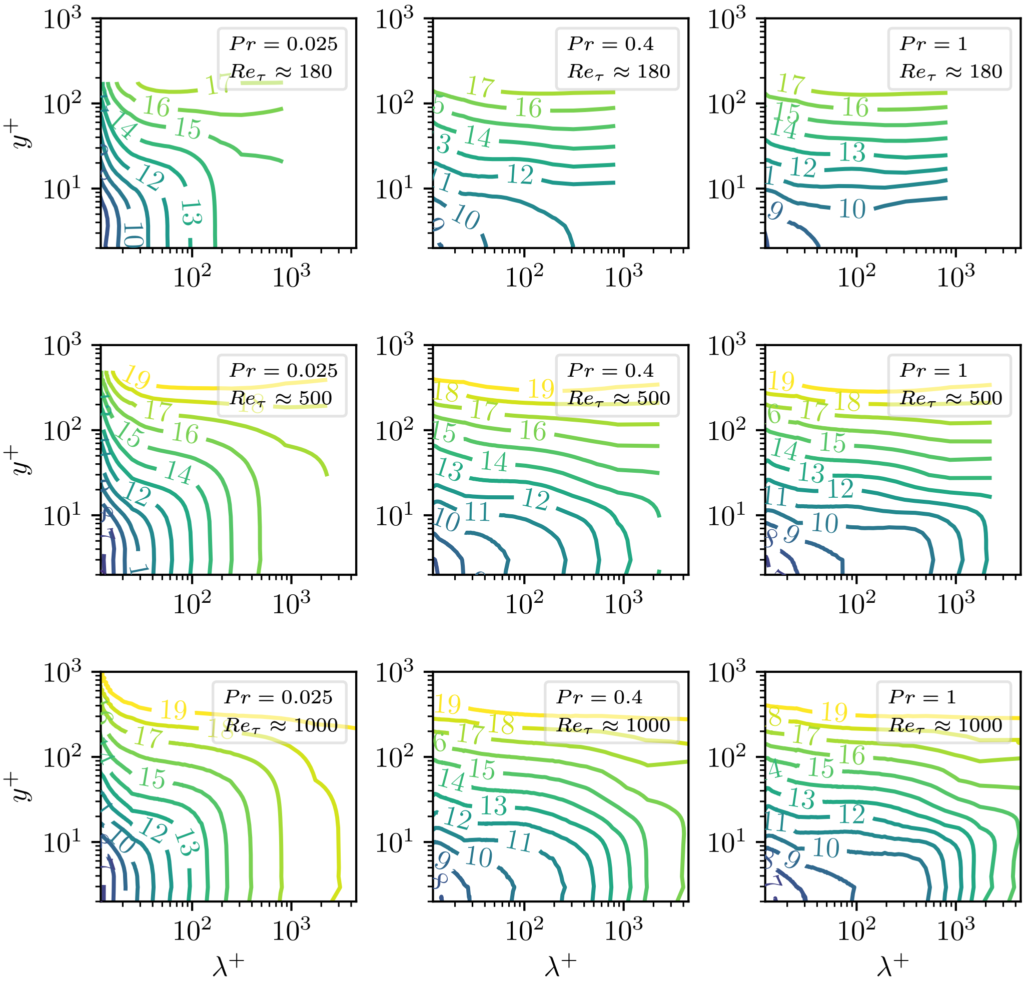

Figure 4. Maps of $U^+_{\mathrm{c},\Theta}(\lambda, y)$ as a function of the isotropic lengthscale $\lambda^+ = 2\pi/k^+$ and the wall normal distance y^+. $U^+_{\mathrm{c},\Theta}(\lambda, y)$ is computed by integrating equation (4) for $\mathscr{K}$ representing a circular wavenumber shell $k = \sqrt{k_x^2 + k_z^2}$ of constant wavenumber vector magnitude. *Pr* increses from left to right, *Re* from top to bottom.

lar wavenumber shell $k = \sqrt{k_x^2 + k_z^2}$ of constant wavenumber vector magnitude. Figure 4 shows $U^+_{\mathrm{c},\Theta}(\lambda, y)$ for the different *Re* and *Pr*-values. A near-wall region of y-independent $U^+_{\mathrm{c},\Theta}(\lambda, y)$ is visible at all λ^+ as approximately vertical contour lines in figure 4. The wall-normal extent of such region increases with λ^+ and is larger for larger λ^+. Moreover, a region farther from the wall where $U^+_{\mathrm{c},\Theta}(\lambda, y)$ becomes approximately, yet not exactly, scale independent can be identified as approximately horizontal contour lines in figure 4. Only for $Pr = 0.025$ $U^+_{\mathrm{c},\Theta}(\lambda, y)$ retains its scale-dependence at all wall-normal distances, with a rapid decline of $U^+_{\mathrm{c},\Theta}(\lambda, y)$ for $\lambda^+ \lesssim 30$ at all y^+.

A more quantitative analysis of these two regions is presented in figure 5, where $U^+_{\mathrm{c},\Theta}(\lambda, y)$ is shown near the wall ($y^+ = 5$) and farther from it ($y^+ = 150$). At $y^+ = 5$, the scale-dependent convection velocity varies mostly with *Pr* and is less dependent on *Re*. For a given *Pr*, it becomes *Re*-independent below a certain value of λ^+, which we observe to be approximately λ^+ *approxRe*$_\tau$ with a tendency to become smaller for smaller *Pr* numbers. A different behaviour is observed at $y^+ = 150$: $U^+_{\mathrm{c},\Theta}(\lambda, y)$ varies mostly with *Re* and depends mildly on *Pr*, differing markedly only for $Pr = 0.025$. The scale-dependence of $U^+_{\mathrm{c},\Theta}(\lambda, y)$ is mild at this wall-normal height. We observe that the λ-behaviour of the scale-dependent convection velocity between the two largest Reynolds numbers is very similar for the two largest *Pr*-numbers and differs mostly by an offset of $U^+_{\mathrm{c},\Theta}$ independent of λ^+.

Finally, we extend the analysis by considering the convection velocity $u_{\mathrm{c},\Theta}(k_x, k_z, y)$ as defined in equation (2), i.e. as function of the streamwise and spanwise wavenumbers, k_x and k_z respectively, and wall-normal distance. Figure 6 shows $u_{\mathrm{c},\Theta}(k_x, k_z, y)$ at $y^+ = 5$, i.e. in the near wall region, for all considered *Pr*- and *Re*-numbers. For clarity, the data is presented as function of $\lambda_x^+ = 2\pi/k_x^+$ and $\lambda_z^+ = 2\pi/k_z^+$ — the streamwise and spanwise wavelenghts — and the $u_{\mathrm{c},\Theta}$ map is smoothed through a moving average with a rolling (3×3)-window applied in the discrete (k_x^+, k_z^+)-space. For all *Pr*- and *Re*-numbers, an area of large statistical noise at $\lambda_x^+ \gg \lambda_z^+$, already observed by del Álamo & Jiménez (2009) for $u_{\mathrm{c},u}$, has been omitted. Its existence is ascribed to a poor convection velocity estimation for very elongated fluctuations, which then feature small gradients along the streamwise direction, in particular if their temporal lifespan is short, as it may be the case for fluctuation with at small λ_z^+.

Figure 6 shows that, while the fluctuation energy is known to be distributed anisotropically, $u_{\mathrm{c},\Theta}$, albeit not exactly, is approximately isotropic, supporting the simplified analysis in terms of a single isotropic wavelength λ^+ of figures 4 and 5.

Regardless of the *Pr*-number, an increase in Re_τ is ac-

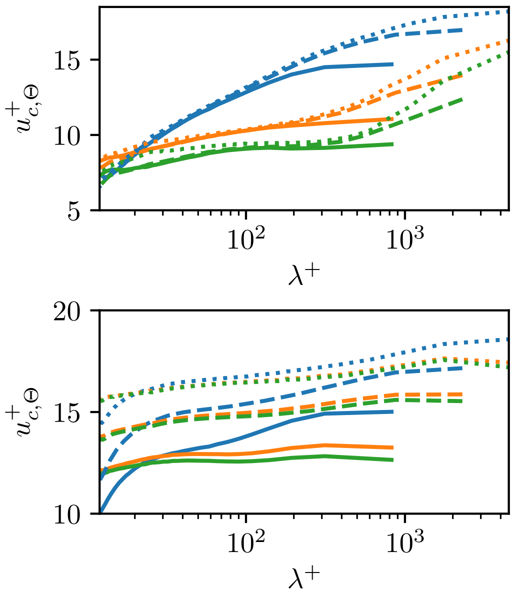

Figure 5. Scale-dependent convection velocity $U^+_{c,\Theta}(\lambda, y)$ of passive scalar fluctuations as a function of the isotropic length-scale $\lambda^+ = 2\pi/k^+$ at $y^+ = 5$ (top) and $y^+ = 150$ (bottom). Line colors denote Pr: —— $Pr = 0.025$; —— $Pr = 0.4$; —— $Pr = 1$. Line styles denote Re_τ: —— $Re_\tau = 180$; - - - $Re_\tau = 500$; ······ $Re_\tau = 1000$.

companied by an increase in the spectral convection velocity, particularly at the larger wavelengths: an observation already made in the context of figure 5. This is visible here as a shift of the respective $u^+_{c,\Theta}$ isolines towards smaller wavelengths with an increase in the Reynolds number. On the other hand, decreasing the Pr-number yields to an increase of $u^+_{c,\Theta}$ at all $(\lambda^+_x, \lambda^+_z)$ and for all Re. This Pr-number effect is additionally emphasised on the global convection velocity by the respective positions of the peaks of the premultiplied energy spectra in dependence of Pr: for $Pr = 0.025$ most fluctuation energy resides within larger, faster-travelling structures, while medium-sized scales hold most of the energy for $Pr = 0.4$ and $Pr = 1$. Even though flows with larger Prandtl numbers contain more passive scalar energy, in general, the respective distribution of it leads to a dominance of faster convected structures in lower-Pr flows. An increase in large-scale energy is visible with larger Reynolds numbers. Due to the definition of equation (3), both changes in $u^+_{c,\Theta}$ and $k^+_x k^+_z \Phi^+_\Theta$ with Reynolds numbers affect the behaviour of the overall convection velocities seen in figure 2. Since these shifts are slightly different for the three Pr-numbers, their effects on the overall convection velocities also differ.

CONCLUSION

This work aimed at shedding light on the behaviour of convection velocity of passive scalar fluctuations, such as small temperature fluctuations, in wall-bounded turbulence at different values of Prandtl (Pr) and Reynolds (Re_τ) number. The results of del Álamo & Jiménez (2009) were chosen as a starting point for the presented research. DNSs of doubly periodic turbulent plane channel flows were conducted at $Re_\tau \in \{180,\ 500,\ 1000\}$ with $Pr \in \{0.025,\ 0.4,\ 1\}$. Close to the channel centre, the overall convection velocities are closely aligned with the mean streamwise velocity profile, while approaching a constant value near the wall due to the footprint of the turbulent eddied located in the buffer layer and further from the wall. The near-wall value of the convection velocity increases with a decrease in Pr, due to the tendency of such flows to form passive scalar fluctuation of larger characteristic lengthscales. In general, the convection velocities of larger scales have been shown to be closer to the bulk velocity, whereas the convection of smaller scales is dominated by the local mean streamwise velocity. The results of Hetsroni *et al.* (2004) were revisited and a deviation from their proposed empirical correlation is found for the convection of passives scalars at $Pr < 1$, and a previously unobserved Re-number dependence. The behaviour of the overall convection velocities has been related to the distributions of the respective spectral convection velocities and energies in the wavenumber space. When computed in terms of a single isotropic wavelength λ^+, the spectral convection velocity does only depend on λ^+ and not on the wall normal distance in a near-wall layer, whose wall-normal extent increases with λ^+ and is generally larger for larger Pr-numbers. Farther from the wall, the opposite occurs: the convection velocity becomes only mildly dependent on the scales and varies mostly with the distance from the wall. The cases with the lowest considered Prandtl number ($Pr = 0.025$) are an exception and preserve a scale dependence, particularly at small λ^+, up towards the channel centre.

These results will be useful to improve the current description and models for the convection velocity of passive scalar fluctuations and can aid the development of thermographic techniques for the convection-velocity-based estimation of wall friction. Future developments should address Prandtl numbers larger than unity at various Reynolds number and expand to different temperature wall boundary condition, such as constant heat flux or conjugate heat transfer. Moreover, the empirical model for the convection velocity developed by del Álamo & Jiménez (2009) should be extended to passsive scalar fluctuations.

REFERENCES

Astarita, T. & Carlomagno, M. 2012 *Infrared Thermography for Thermo-Fluid-Dynamics*, 2nd edn. Springer Berlin, Heidelberg.

Choi, H. & Moin, P. 1990 On the space-time characteristics of wall-pressure fluctuations. *Physics of Fluids A* **2**, 1450–1460.

Cui, G. & Jacobi, I. 2024 Variability of convection velocities and structure inclination angles in wall-bounded turbulence. *Journal of Fluid Mechanics* **989**, A16.

Goldschmidt, V., Young, M. & Ott, E. 1981 Turbulent convective velocities (broadband and wavenumber dependent) in a plane jet. *Journal of Fluid Mechanics* **105**, 327–345.

Hetsroni, G., Tiselj, I., Bergant, R., Mosyak, A. & Pogrebnyak, E. 2004 Convection velocity of temperature fluctuations in a turbulent flume. *Journal of Heat Transfer* **126**, 843–848.

Hussain, F. & Clark, R. 1980 Measurements of wavenumber-celerity spectrum in plane and axisymmetric jets. *AIAA Journal* **19**, 51–55.

Jeon, S., Choi, H., Yoo, J. & Moin, P. 1999 Space-time characteristics of the wall shear-stress fluctuations in a low-reynolds-number channel flow. *Physics of Fluids* **11**, 3084–3094.

Khoo, B., Chew, Y. & Teo, C. 2001 Near-wall hot-wire measurements . part ii: Turbulence time scale, convective velocity and spectra in the viscous sublayer. *Experiments in*

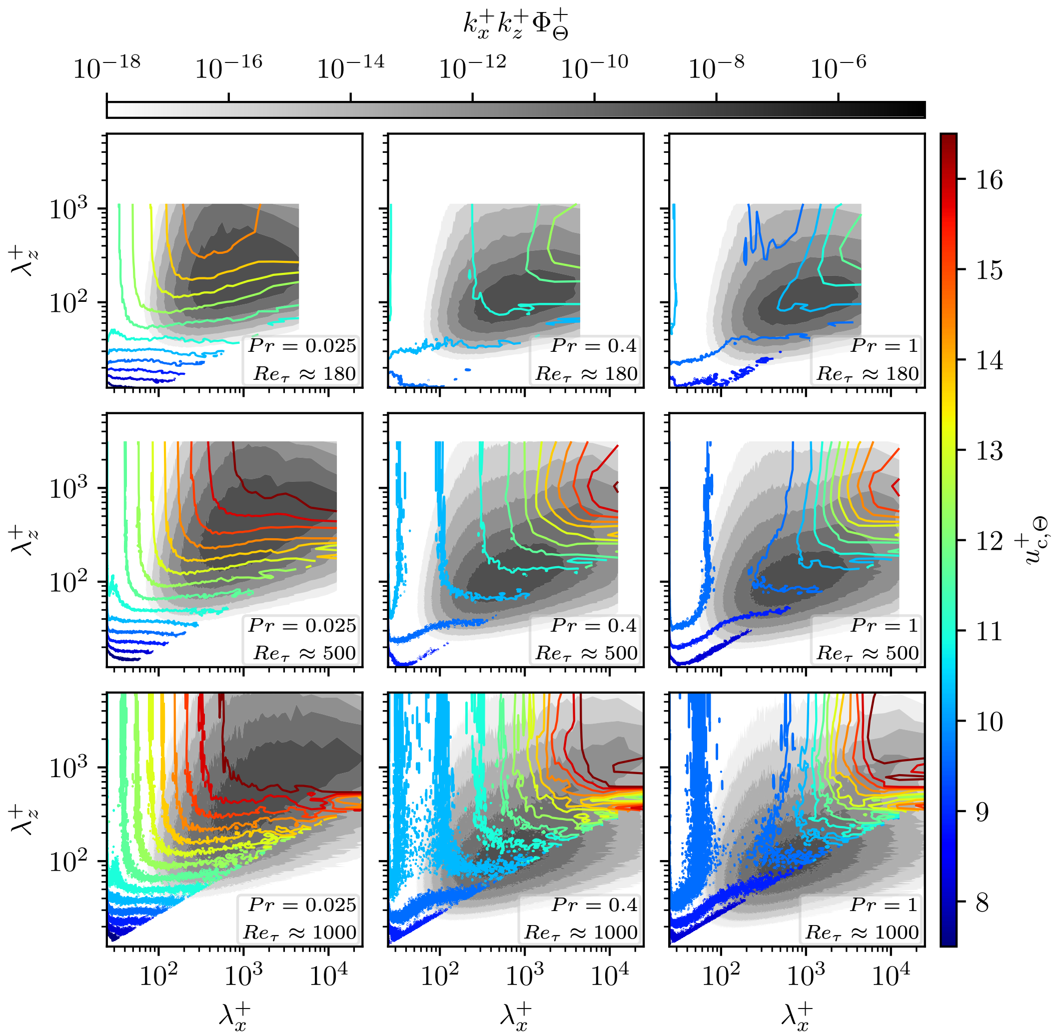

Figure 6. Distributions of the premultiplied energy spectra and spectral convection velocities of passive scalar fluctuations in viscous units. Data are shown at $y^+ = 5$.

Fluids **31**, 494–505.

Kim, J. & Hussain, F. 1993 Propagation velocity of perturbations in turbulent channel flow. *Physics of Fluids* **5**, 695–706.

Kowalewski, T., Mosyak, A. & Hetsroni, G. 2003 Tracking of coherent thermal structures on a heated wall. *Experiments in Fluids* **34**, 390–396.

Liu, T., Chen, T. & Miozzi, M. 2023 Correlation between skin friction and enstrophy convection velocity in near-wall turbulence. *European Journal of Mechanics - B/Fluids* **104**, 224–230.

Liu, T., Sullivan, J. P., Asai, K., Klein, C. & Egami, Y. 2021 *Pressure- and Temperature-Sensitive Paints*, 2nd edn. Springer Cham.

Liu, T. & Woodiga, S. 2011 Feasibility of global skin friction diagnostics using temperature sensitive paint. *Measurement Science & Technology* **22**.

Luchini, P. & Quadrio, M. 2005 A low-cost parallel implementation of direct numerical simulation of wall turbulence. *Journal of Computational Physics* **211**, 551–571.

Miozzi, M. & Costantini, M. 2021 Temperature and skin-friction maps on a lifting hydrofoil in a propeller wake. *Measurement Science and Technology* **32**, 114007.

Moin, P. 2009 Revisiting taylor's hypothesis. *Journal of Fluid Mechanics* **640**, 1–4.

Pirozzoli, S., Bernardini, M. & Orlandi, P. 2016 Passive scalars in turbulent channel flow at high reynolds number. *Journal of Fluid Mechanics* **788**, 614–639.

Quadrio, M. & Luchini, P. 2003 Integral space–time scales in turbulent wall flows. *Physics of Fluids* **15**, 2219–2227.

Renard, N. & Deck, S. 2015 On the scale-dependent turbulent convection velocity in a spatially developing flat plate turbulent boundary layer at reynolds number retheta = 13 000. *Journal of Fluid Mechanics* **775**, 105–148.

Romano, G. 1995 Analysis of two-point velocity measurements in near-wall flows. *Experiments in Fluids* **20**, 68–83.

Taylor, G. 1938 The spectrum of turbulence. *Proceedings of The Royal Society A: Mathematical, Physical and Engineering Sciences* **164**, 476–490.

Wills, J. 1964 On convection velocities in turbulent shear flows. *Journal of Fluid Mechanics* **20**, 417–432.

Zaman, K. B. M. Q. & Hussain, F. 1981 Taylor hypothesis and large-scale coherent structures. *Journal of Fluid Mechanics* **112**, 379–396.

del Álamo, J. C. & Jiménez, J. 2009 Estimation of turbulent convection velocities and corrections to taylor's approximation. *Journal of Fluid Mechanics* **640**, 5–26.